IETI Transactions on Engineering Research and Practice
http://ieti.net/TERP/

2018, Volume 2, Issue 2, 56-67, DOI 10.6723/TERP.201812_2(2).0008

STUDY OF THE INFLUENCE OF CYCLE FACTORS ON THE THERMAL FATIGUE BEHAVIOR OF ALUMINUM ALLOY 2017A

Lamine Rebhi [1, a], Branimir Krstic [2,b], Boudiaf Achraf [1,c], Aderraouf Zemmoura [1,d], Dragan Trifkovic [2,e]

[1]Laboratoire Génie des Matériaux, Ecole Militaire Polytechnique, BP 17 Bordj El-Bahri Alger, Algeria,
[2]Military academy University of Defence in Belgrade, Belgrade, Serbia,
[a]rebhi.lamine@gmail.com, [b]branimir.krstic@va.mod.gov.rs, [c]achraf_boudiaf@yahoo.fr,
[d]z.abderraouf1989@gmail.com, [e]dragan.trifkovic@va.mod.gov.rs.

Abstract The severe operating conditions under cyclic variation in temperature and constraints have exposed many industrial components to the phenomenon of thermal fatigue. In order to study the behavior of the aluminum alloy 2017A in thermal fatigue, the alloy is submitted to a cyclic thermal load. The effect of cycling in temperature on the macroscopic behavior were observed through the changes of the microstructure. Two important parameters of thermal cycles were taken into account; the first is the maximum temperature Tmax reached in a cycle. The second factor considered is the number of cycles applied. The results show a softening when the number of cycle increases. This evolution is accentuated when Tmax is high. This fall of hardness is due to the decomposition of the precipitates, which is responsible of the hardening of material.

Keywords: 2017A Aluminum alloy; thermal fatigue; microstructure; softening.

1. INTRODUCTION

Thermal fatigue is an almost ubiquitous phenomenon in our environment both in everyday life and in the industrial field. In fact, fluctuations in temperature, whether seasonal, weekly, daily, or more frequent, have a damaging character because these fluctuations are repeated over time. Let's briefly mention some examples: the peeling of the paint due to coupled effects of variation of humidity and temperature, the cracks that form at the bottom of a coffee cup due to the many fillings of hot liquid in a cup whose walls are significantly colder.

In most cases, the mechanical parts are designed to withstand static mechanical loadings or, at best, mechanical fatigue. It is sometimes found that these parts are subject to significant temperature variations that can cause the material to break down by cracking and prematurely ruin these parts. The phenomenon is commonly called thermal fatigue.

An example illustrating the effects of thermal fatigue is given below in the nuclear field, which represents a significant part of the electricity production. However, its exploitation presents a lot of risks, in particular the problem of radioactive fluid leaks. In 1998, on the site of the Civaux nuclear power plant located in the department of Vienne, a leak was observed on the weld seam of the mixing tee of the hot and cold fluids of the secondary cooling circuit. After expertise, a crack opening 180 mm long on the outer skin of the elbow was detected. In addition, cracking networks with cracks limited to 2-3mm in depth were observed. The appearance of the networks of cracking made it possible to conclude that this leak had for origin, the thermal fatigue [1].

2018, Volume 2, Issue 2, 56-67, DOI 10.6723/TERP.201812_2(2).0008

In order to enhance understanding of thermal fatigue phenomenon, many studies were conducted. A comparative study on the change of microstructure under thermal loading of two aluminum alloys was presented in details in [2]. The conducted study consists in applying a cyclic thermal loading on the two aluminum alloys 2017A and 4047. A change in the mechanical properties reflected by a drop in hardness as a function of the number of cycles was observed in both alloys due to microstructural changes.

Sasaki in reference [3] reproduced in his thermal fatigue tests on the aluminum alloy 319(according to ASTM designation system), work-conditions under which cylinder head of a diesel motor are subjected. After the thermal fatigue tests, two types of precipitates were observed and categorized into needle-like and ellipsoidal-like. This study led to the conclusion that thermal fatigue life is influenced by temperature range, cycle period, strain range, and mean strain.

The purpose of this work is to give a contribution by an experimental study of the thermal fatigue behavior of the 2017A aluminum alloy. Our main objective is to study the effect of heating and cooling cycles on the microstructure of the chosen alloy. A thermal fatigue device designed at the Laboratory Materials Engineering ensures the temperature cycling. Two parameters are considered, namely: cycle number and maximum heating temperature.

2.PRESENTATION OF THE STUDY MATERIAL

2.1. Chemical Composition and Mechanical Properties

The material used in the study is the aluminum alloy 2017A. The analysis of the chemical composition of the alloy was carried out by means of SPECROLAB spectrometer. The analysis revealed the chemical composition presented in Table 1. which is equivalent to the standard specification for A2017 aluminum alloy taken from [4].

Table 1. Chemical analysis results (wt%).

Element	Result
Copper (Cu)	4.339
Manganese (Mn)	0.586
Iron (Fe)	0.700
Silicon (Si)	0.990
Zinc (Zn)	0.211
Magnesium (Mg)	0.931
Aluminum (Al)	Bal.

The mechanical properties of the study material are shown in Table 2.

Table 2. Mechanical properties of the 2017A aluminum alloy [4].

Mechanical properties	Result
Yield strength Re [MPa]	4.339
Tensile strength Rm [MPa]	0.586
Elongation A (%)	0.700
Hardness (HV)	0.990

IETI Transactions on Engineering Research and Practice
http://ieti.net/TERP/

2018, Volume 2, Issue 2, 56-67, DOI 10.6723/TERP.201812_2(2).0008

2.2.Metallographic Observation of the Study Material in the As-received Condition

The preparation of a sample of the material for microscopic examination consists of sampling, coating, polishing and finally, chemical etching by the Keller reagent. As the material is delivered in the form of extruded bars, Metallographic preparation of longitudinal and transverse sections to the rolling direction were performed. Figure 1. shows the results of the optical micrographic observation.

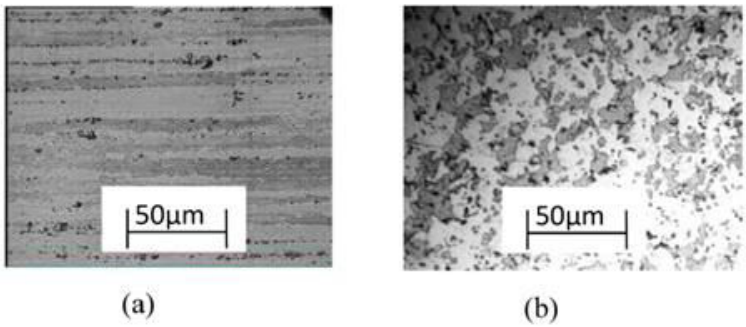

Figure 1. Micrograph of the alloy 2017A: (a) longitudinal section and (b) transversal section.

3.THERMAL FATIGUE TESTS

3.1. Specimen Geometry

The thermal fatigue tests were carried out on tubular cylindrical specimens with a thickness of 2 mm (in the useful zone). The specimens were taken and machined from cylindrical bars of dimensions Φ30×130mm. Figure 2. shows the geometry and the dimensions of the test specimen.

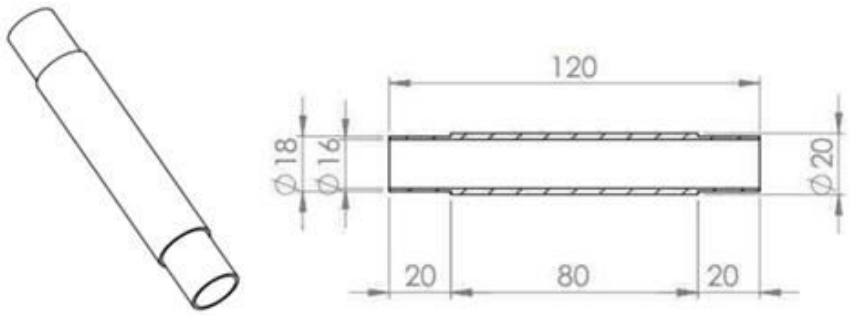

Figure 2. Geometry and dimensions of the thermal fatigue test specimen.

3.2. Experimental Procedure

The thermal fatigue device used exploits the principle of joule heating. An electric furnace with a nominal power of 1000W allowing to reach the temperatures of the order of 500 ° C on the outer surface of the specimen. Cooling is achieved by circulating water inside the specimen (tube) with a constant flow rate of 7.5 l / min, and the face is exposed to the open air and cooling is obtained therefore, by Natural convection. A schematic representation of the device is shown in Figure 3.

IETI Transactions on Engineering Research and Practice
http://ieti.net/TERP/

2018, Volume 2, Issue 2, 56-67, DOI 10.6723/TERP.201812_2(2).0008

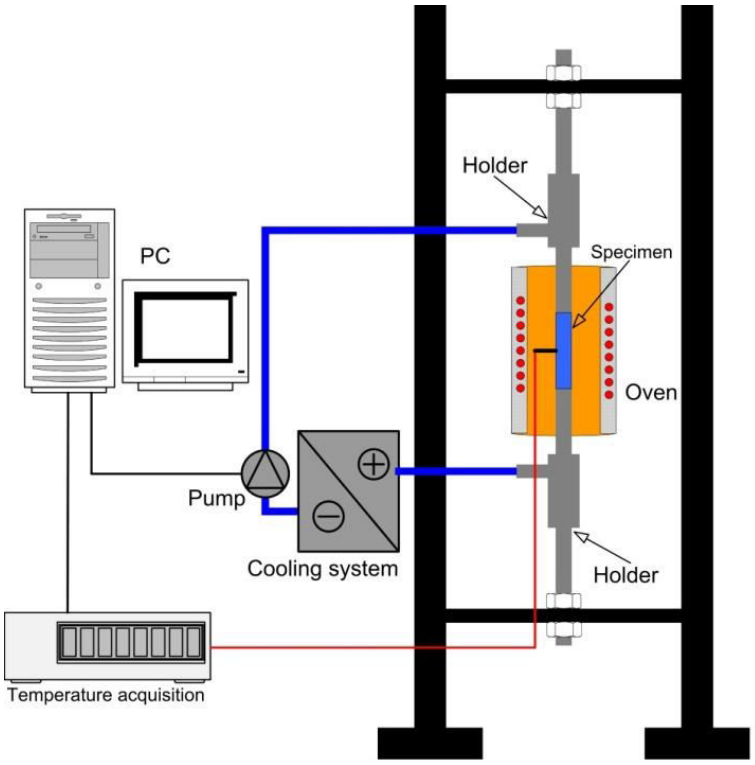

Figure 3. Schema of the thermal fatigue test device.

Given the time of a cycle; relatively high (more than three minutes), a moderately fast data acquisition system with microcomputer data storage was developed. This microcomputer is linked to a SCXI-1000 signal conditioner that amplifies weak signals, isolates them and filters them to obtain more precise measurements.

An interface for data acquisition was developed with LabView software. It ensures the acquisition and continuous recording, over several channels, the temperature as a function of time. The thermocouple used is of type K, of diameter 0.1 mm, glued on the external surface of the specimen in the middle of the useful part.

In order to follow the evolution of the temperature over time, we glued a thermocouple of type k of diameter 0.1mm on the external surface of the specimen in the middle of the useful part. The thermal cycles obtained on the outer surface of the test piece are shown in Figure 4. The control of the temperature of the furnace is done by another thermocouple.

The cycling in temperature is done without the intervention of the operator. Simply specify the setpoint values (Tmax and Tmin) on the control interface and start the test. As soon as the temperature of the specimen reaches the value Tmax, the water pump starts automatically to ensure the cooling of the specimen to the temperature Tmin.

IETI Transactions on Engineering Research and Practice
http://ieti.net/TERP/

2018, Volume 2, Issue 2, 56-67, DOI 10.6723/TERP.201812_2(2).0008

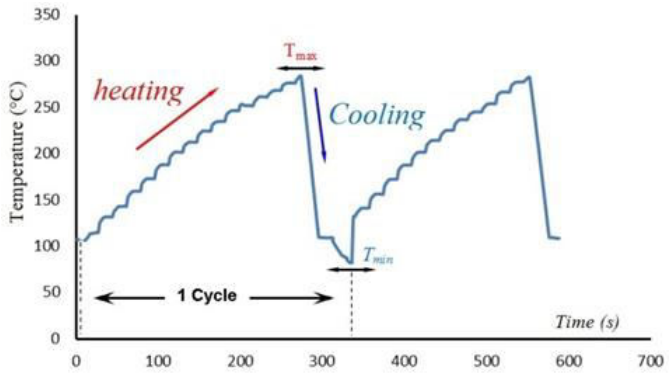

Figure 4. Thermal cycles applied to the thermal fatigue specimen.

During cooling, the oven remains energized in order to minimize heating time during the next cycle.

Table 3. presents all the thermal cycles adopted in this study. The minimum temperature of the thermal cycle (T_{min}) was kept constant at 80 ° C for all tests, while the maximum temperature (T_{max}) was varied between 200°C and 280°C.

Table 3. Adopted thermal cycles.

Oven power [W]	**1000**
Tmin [°C]	80
Tmax [°C]	200-280
Heating time [s]	210-300
Cooling time [s]	35-45

There are two types of tests, commonly called "interrupted" and "continuous" tests. The interrupted tests are used to follow the evolution of mechanical properties in the surface of the specimens during cycling (oxide layer, hardness, etc.). Continuous tests are destructive and allow the termination of softening and changes in microstructures. In our case, continuous type tests are performed. Table 4. shows the number of cycles at a standstill for the continuous tests considered in this study.

Table 4. Number of cycles at the end of thermal fatigue tests.

Tmax [°C]	**Duration of thermal cycle [s]**	**Number of cycles**		
200	210	1000		5000
280	300	10	1000	3000

4. RESULTS AND INTERPRETATIONS

4.1. Influence of Thermal Cycling Factors on Hardness

In order to study the influence of thermal fatigue on the mechanical properties of aluminum alloy 2017A, hardness tests on different specimen having undergone different cycling are carried out, in other words, different number of cycles at different maximum temperatures Tmax. Hardness tests are realised by indentation of a Vickers indenter with a load of 30 kg. The results obtained are shown in Figure 5.

IETI Transactions on Engineering Research and Practice
http://ieti.net/TERP/

2018, Volume 2, Issue 2, 56-67, DOI 10.6723/TERP.201812_2(2).0008

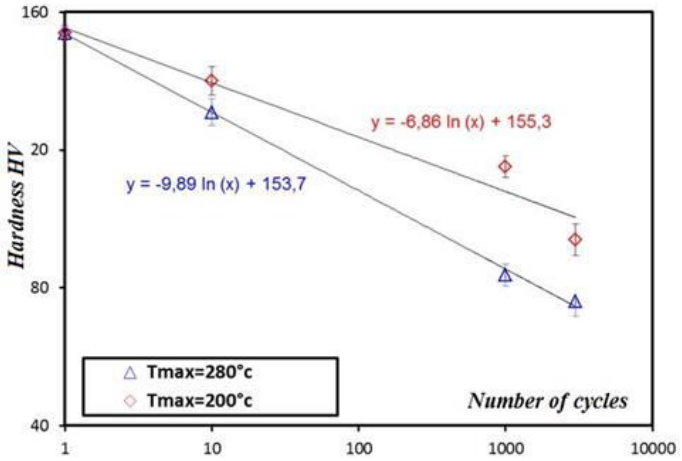

Figure 5. Evolution of hardness as a function of cycle number and T_{max}.

It can be observed from the results, that the hardness decreases linearly with ln (N), and this evolution is more pronounced for the tests at Tmax = 280 ° C, the trend curve passes virtually by all points.

It should be noted that the hardness difference between the tests at 200°C and 280°C becomes larger when ln (N) increases. This difference can be seen after 10 cycles only, the hardness goes from 154(HV) in the initial state up to 140(HV) at Tmax = 200°C, and it reaches 131 (HV) at Tmax = 280°C

To be able to interpret the results obtained, it is preferable to have a prior idea of probable events.

The hardness drop is probably due to the following:

- Migration of the precipitates towards the core of the part in this case Al2Cu precipitates which are harder than pure aluminum (α phase),
- Migration of precipitates to grain boundaries,
- Reduction in the total area of the grain boundaries,
- Movement of dislocations,
- Increase in the number of gaps.

The third hypothesis is ignored since the chemical etching done has not allowed us to see grain boundaries for samples with a high number of cycles. As the means of characterization put at our disposal do not allow us to verify hypotheses four and five, the only possibilities that remain are the first and the second.

To identify the exact cause that led to the hardness decrease, an analysis of the microstructure at different stages of thermal fatigue must be performed, which allows a correlation between the micro and macroscopic properties of our alloy.

IETI Transactions on Engineering Research and Practice
http://ieti.net/TERP/

2018, Volume 2, Issue 2, 56-67, DOI 10.6723/TERP.201812_2(2).0008

4.2. Influence of Thermal Cycling Factors on Precipitation Rate

Samples taken from several specimens in various directions and at different numbers of cycles and different temperatures (Tmax), are visualized by high- performance scanning electron microscope (SEM), the images obtained are set out below.

The 2017A alloy at the initial state: The SEM micrpgraph of the alloy 2017A Figure 6. indicates that the alloy structure is formed of aluminum crystals in solid solution (white) with Al2Cu (θ) insertion (light gray) and other types of precipitates in segregations.

The 2017A alloy after 10 cycles at Tmax = 280°C: As seen previously, the hardness decreased after only 10 cycles. By comparing the cross-sectional and longitudinal section of the sample taken Figure 7.(a) and Figure 7.(b), it is noted that the distribution of the precipitates is the same in both directions, which makes it possible to eliminate the hypothesis of the depletion of the Al2Cu surface.

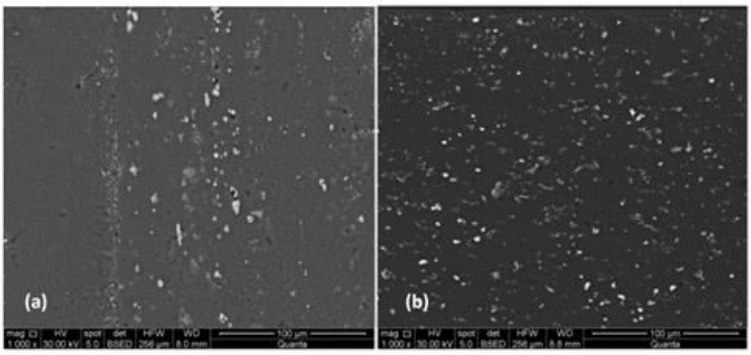

Figure 6. SEM micrograph indicating the constituent particles of the 2017A alloy at the initial state: (a) longitudinal section and (b) transversal section.

By comparing the microstructure of the alloy at initial state and after 10 cycles, it can be noted that there is no change in the microstructure or in the size of the precipitates; therefore the decrease in the hardness is mainly due to the increase of the number of pores [5]. The increase of the number of pores results from the rise in temperature during the heating phase [6].

The increase in the number of pores as a function of temperature is governed by the following equation:

$$n_L = Ne^{-\frac{E}{KT}} \tag{1}$$

Where:

n_L pore concentration per unit volume,

N number of atoms per unit volume

E energy of formation of pores,

IETI Transactions on Engineering Research and Practice
http://ieti.net/TERP/

2018, Volume 2, Issue 2, 56-67, DOI 10.6723/TERP.201812_2(2).0008

K Boltzmann constant,

T absolute temperature [K].

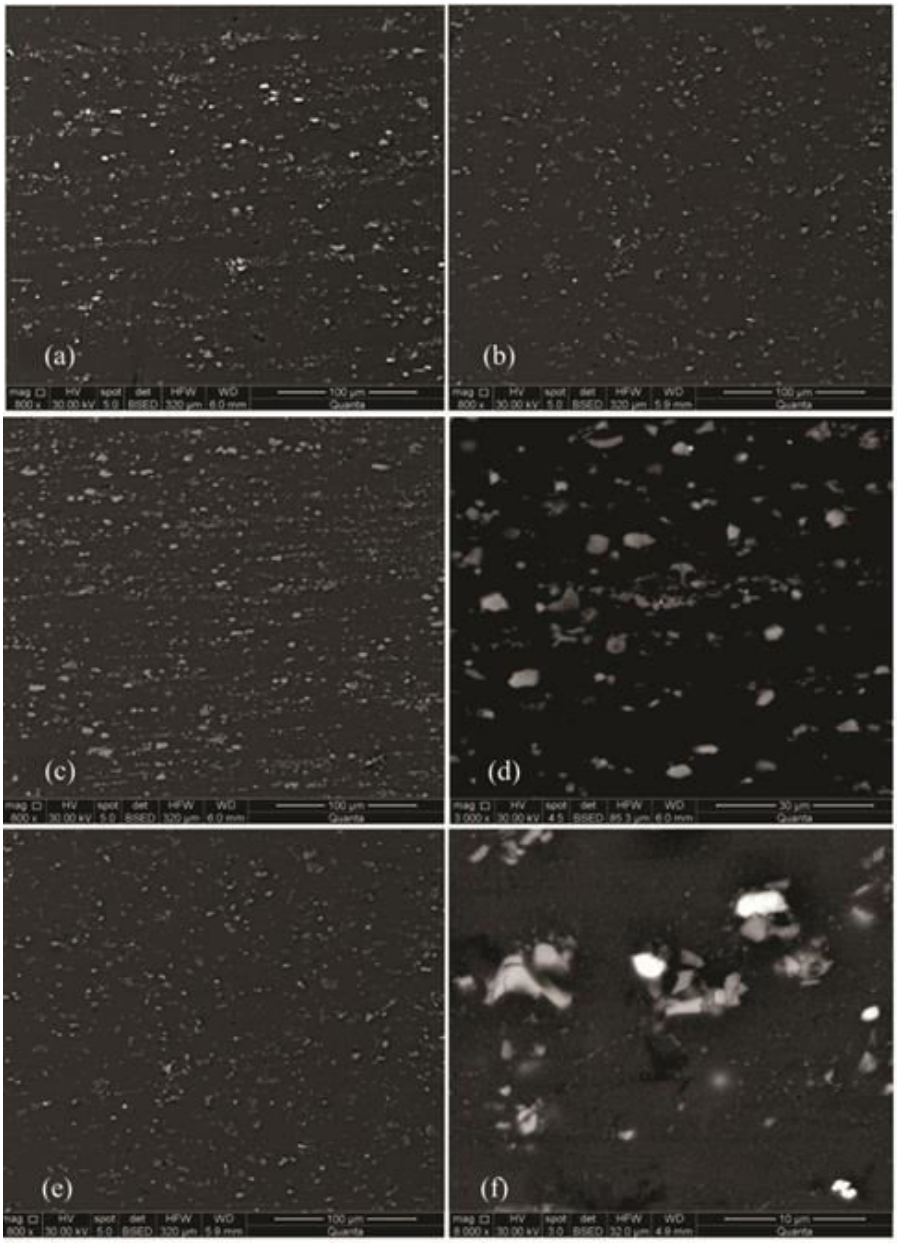

Figure 7. SEM images of the 2017A alloy after thermal fatigue tests with T_{max}=280°C: (a) longitudinal section after 10 cycles; (b) transversal section after 10 cycles; (c) and (d) after 1000 cycles; (e) and (f) after 3000 cycles.

IETI Transactions on Engineering Research and Practice
http://ieti.net/TERP/

2018, Volume 2, Issue 2, 56-67, DOI 10.6723/TERP.201812_2(2).0008

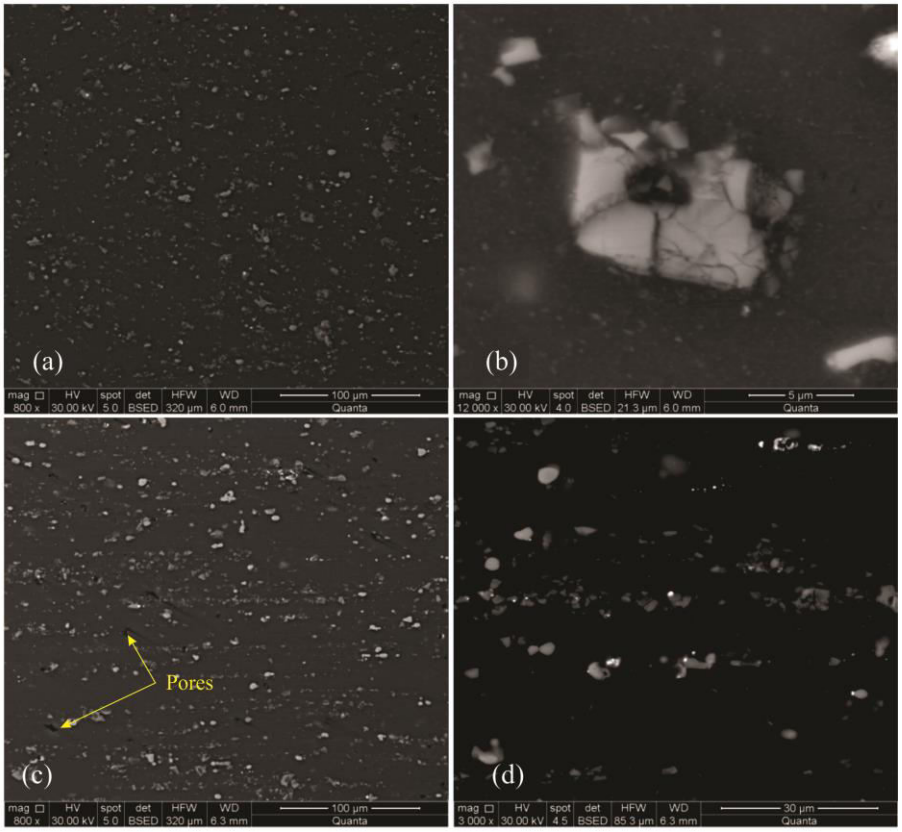

Figure 8. SEM images of the 2017A alloy after thermal fatigue tests with T_{max}=200°C: (a) and (b) after 1000 cycles; (c) and (d) after 5000 cycles.

The 2017A alloy after 1000 cycles at Tmax = 280°C: By comparing the alloy after 1000 cycles with the initial state, it can be observed a change in size and in the distribution of precipitates. By carrying out a larger magnification, it is noted that there is a decomposition of the precipitates Al2Cu (θ). Referring to the Al-Cu binary equilibrium diagram in Figure 9. each time the material is brought to a temperature of 280°C the portion (A) which is shown in Figure 9. dissolves and the percentage of the dissolve portion can be determine by the rule of the inverse segments.

The 2017A alloy after 3000 cycles at Tmax = 280°C: The findings that can be drawn from Figure 7.(f) is that the decomposition of precipitates Al2Cu (θ) continues; therefore, their sizes are much finer.

The alloy 2017A after 1000 cycles at Tmax = 200°C: The decomposition of the precipitates Al2Cu is always noted Figure 8.(a) and Figure 8.(b) , nevertheless As this time the heating temperature is lower than the first, the fraction dissolved at each cycle is less important.

The 2017A alloy after 5000 cycles and Tmax = 200°C: After 5000 cycles, the appearance of pores, which are the preferred sites for the formation of microcracks Figure8.(c).

IETI Transactions on Engineering Research and Practice
http://ieti.net/TERP/

2018, Volume 2, Issue 2, 56-67, DOI 10.6723/TERP.201812_2(2).0008

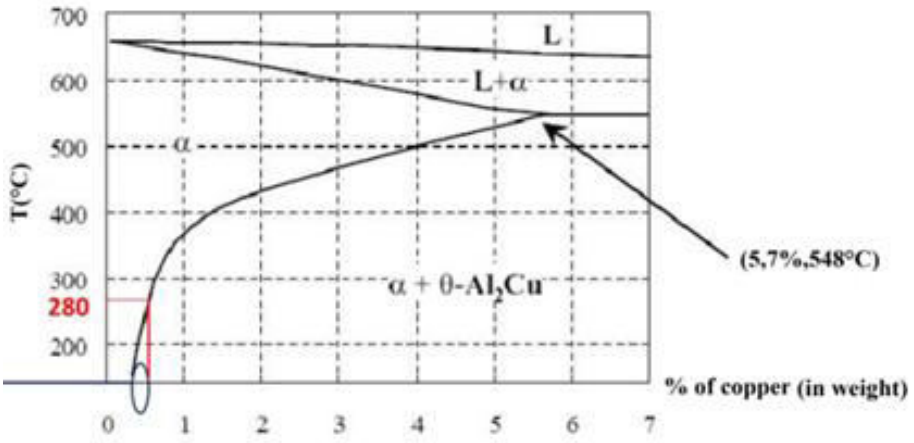

Figure 9. Aluminum-rich part of the Al-Cu equilibrium diagram [7].

The micrographs of the samples taken were obtained in (BSE) which means in backscattered electrons, these images in contrast 'Z' make it possible to give a relief in phase contrast, the phases which consist mainly of heavy elements appear in contrast white while the phases formed of light elements appear in dark contrast. This phase contrast allowed us to distinguish four phases in all, a matrix in dark gray as well as three types of precipitates under different color contrast Figure 10. Thanks to these images obtained it was possible to carry out a chemical composition analysis with the help of the EDS analyzer, of the four phases present Figure 11.

In order to determine the nature of the precipitates (1), (2) and (3), a XRD analysis was performed on the different samples Figure 12. We were able to confirm the presence of two precipitates, the precipitate 2 as AlCuMg and the precipitate 3 as Al2Cu. The first precipitate does not appear on the diffractograms, this is probably due to: the coarse scan step, the resemblance of the mesh parameters between the different precipitates and the matrix.

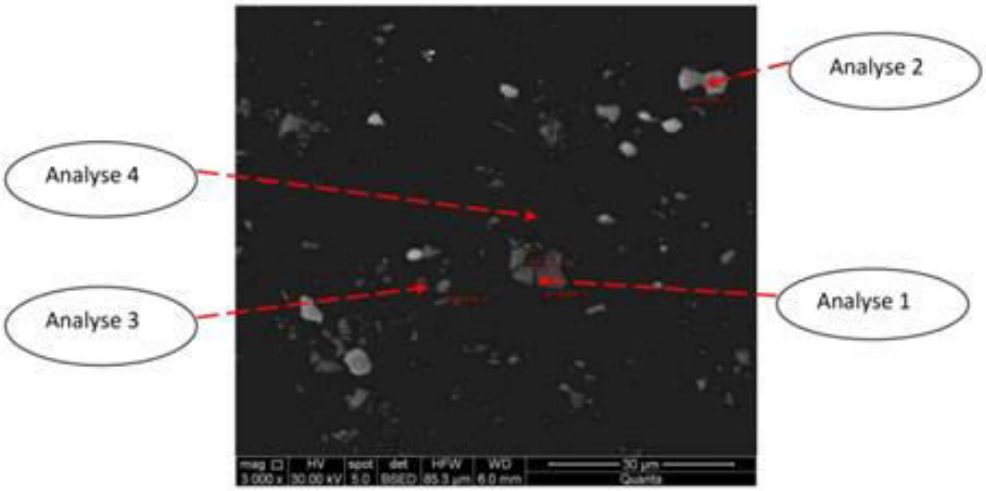

Figure 10. Phases present in the alloy 2017A.

IETI Transactions on Engineering Research and Practice
http://ieti.net/TERP/

2018, Volume 2, Issue 2, 56-67, DOI 10.6723/TERP.201812_2(2).0008

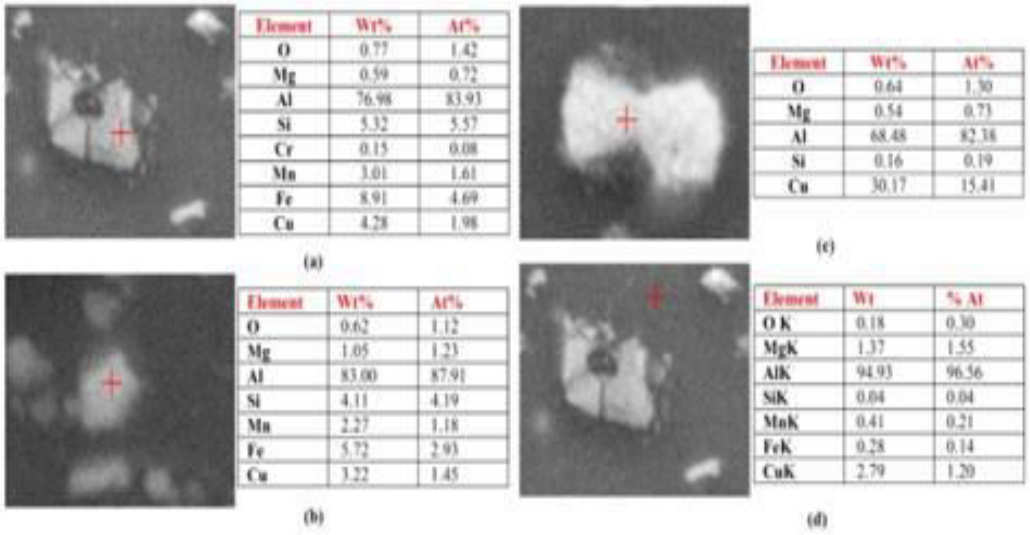

(a)

Element	Wt%	At%
O	0.77	1.42
Mg	0.59	0.72
Al	76.98	83.93
Si	5.32	5.57
Cr	0.15	0.08
Mn	3.01	1.61
Fe	8.91	4.69
Cu	4.28	1.98

(c)

Element	Wt%	At%
O	0.64	1.30
Mg	0.54	0.73
Al	68.48	82.38
Si	0.16	0.19
Cu	30.17	15.41

(b)

Element	Wt%	At%
O	0.62	1.12
Mg	1.05	1.23
Al	83.00	87.91
Si	4.11	4.19
Mn	2.27	1.18
Fe	5.72	2.93
Cu	3.22	1.45

(d)

Element	Wt	% At
O K	0.18	0.30
MgK	1.37	1.55
AlK	94.93	96.56
SiK	0.04	0.04
MnK	0.41	0.21
FeK	0.28	0.14
CuK	2.79	1.20

Figure 11. Different phases in the 2017A alloy with EDS microanalysis: (a) Precipitated1. (b) Precipitated2. (c)Precipitated3. (d) Matrix.

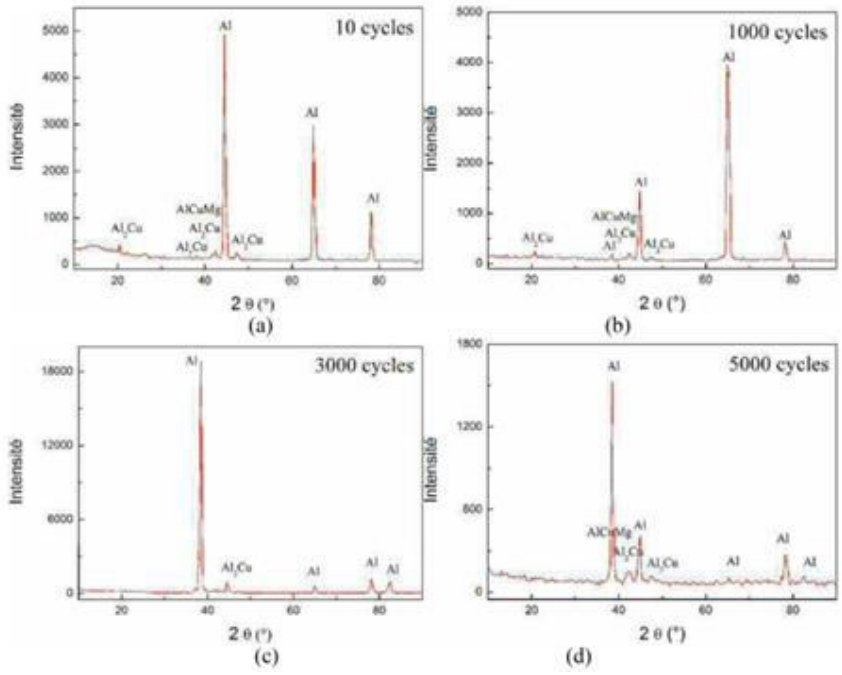

Figure 12. XRD spectra of the samples taken from the test specimens tested in fatigue thermal.

5.CONCLUSION

The objective of this work is to observe the effects of temperature cycling on the macroscopic behavior through changes in the microstructure. Two important parameters of thermal cycles were taken into consideration; the first is the maximum temperature reached in one cycle. The second factor considered is the number of cycles applied.

2018, Volume 2, Issue 2, 56-67, DOI 10.6723/TERP.201812_2(2).0008

For this purpose, thermal fatigue tests on 2017A aluminum alloy specimens were carried out. The results of these tests showed:

- A softening as the number of cycles increases. That evolution is more pronounced when Tmax is higher,
- Supported by XRD analysis and SEM micrograph, we were able to determine that this drop in hardness is due to the decomposition of precipitates, responsible for hardening of the material, present in the matrix. This decomposition of the precipitates will increase the resistance to fatigue.

References

[1] Maillot V., Fissolo A., Degallaix G., and Degallaix S., 2005, Thermal fatigue crack networks parameters and stability: an experimental study, *International Journal of Solids and Structures,* 42, p.p.759–769.

[2] Belkharchouche A., Boudiaf A., and Belouchrani M.E.A., 2017, A comparison between 2017A and 4047A aluminum alloys microstructure changes under thermal fatigue loading, *Materials Science and Engineering: A*, Volume 689, p.p. 96-102.

[3] Sasaki K., and Takahashi T., 2006, Low cycle thermal fatigue and microstructural change of AC2B − T6 aluminum alloy, *International Journal of Fatigue*, 28 (3), p.p. 203–210.

[4] Nunes R.et al, 1990, Properties and Selection. Nonferrous Alloys and Special-Purpose Materials, Vol. 2. ASM International.

[5] Arami H., Khalifehzadeh R., Akbari M., and Khomamizadeh F., 2008, Microporosity control and thermal-fatigue resistance of (A319) aluminum foundry alloy, *Materials Science and Engineering: A*, 472 (1–2), p.p. 107–114.

[6] Roy N., 1994, Etude paramétrique de l'évolution de la porosité dans le système Al-9%Si-3%Cu, thèse de doctorat, université du QUEBEC.

[7] D'Elia F., Ravindran C., Sediako D., Donaberger R., 2015, Solidification analysis of Al–5 wt-%Cu alloy using in situ neutron diffraction, *Canadian Metallurgical Quarterly*, Vol. 54 No 1, p.p. 9-15.